ISSN 1063-7834, Physics of the Solid State, 2011, Vol. 53, No. 10, pp. 2032–2037. © Pleiades Publishing, Ltd., 2011.
Original Russian Text © A.V. Malakhovskii, E.V. Eremin, D.A. Velikanov, A.V. Kartashev, A.D. Vasil'ev, I.A. Gudim, 2011, published in Fizika Tverdogo Tela, 2011, Vol. 53, No. 10, pp. 1929–1934.

MAGNETISM

Magnetic Properties of the $Nd_{0.5}Gd_{0.5}Fe_3(BO_3)_4$ Single Crystal

A. V. Malakhovskii[a, *], E. V. Eremin[a], D. A. Velikanov[a, b], A. V. Kartashev[a], A. D. Vasil'ev[a], and I. A. Gudim[a]

[a] *Kirensky Institute of Physics, Siberian Branch, Russian Academy of Sciences, Akademgorodok, Krasnoyarsk, 660036 Russia*

* *e-mail: malakha@iph.krasn.ru*

[b] *Siberian Federal University, pr. Svobodnyi 79, Krasnoyarsk, 660041 Russia*

Received March 21, 2011

Abstract—The magnetic properties of the $Nd_{0.5}Gd_{0.5}Fe_3(BO_3)_4$ single crystal have been studied in principal crystallographic directions in magnetic fields to 90 kG in the temperature range 2–300 K; in addition, the heat capacity has been measured in the range 2–300 K. It has been found that, below the Néel temperature $T_N = 32$ K down to 2 K, the single crystal exhibits an easy-plane antiferromagnetic structure. A hysteresis has been detected during magnetization of the crystal in the easy plane in fields of 1.0–3.5 kG, and a singularity has been found in the temperature dependence of the magnetic susceptibility in the easy plane at a temperature of 11 K in fields $B < 1$ kG. It has been shown that the singularity is due to appearance of the hysteresis. The origin of the magnetic properties of the crystal near the hysteresis has been discussed.

DOI: 10.1134/S1063783411100180

1. INTRODUCTION

Studies of rare-earth ferroborates $RFe_3(BO_3)_4$ (R = Y, La–Lu) are of interest mainly owing to two circumstances. First, some representatives of this family, e.g., $GdFe_3(BO_3)_4$, $NdFe_3(BO_3)_4$, $PrFe_3(BO_3)_4$, and $HoFe_3(BO_3)_4$, are multiferroics [1–5]; i.e., they simultaneously exhibit magnetic and electric orders. Second, ferroborates of this type have various magnetic structures and undergo different phase transitions depending on the kind of rare-earth ion [6]. It is reasonable to expect that the properties of the $Nd_{0.5}Gd_{0.5}Fe_3(BO_3)_4$ single crystal under study occupy an intermediate position between the properties of the $GdFe_3(BO_3)_4$ and $NdFe_3(BO_3)_4$ crystals. Both crystals have the huntite structure with symmetry $R32(D_3^7)$ at room temperature. The $NdFe_3(BO_3)_4$ crystal retains this structure down to a temperature of 1.6 K [7], and the $GdFe_3(BO_3)_4$ crystal undergoes the structural phase transition to symmetry $P3_121(D_3^4)$ at a temperature of 156 K [8, 9].

The magnetic properties of $GdFe_3(BO_3)_4$ were studied in [10–12]. In the paramagnetic region, the susceptibility follows the Curie–Weiss law with the constant $\Theta = -115$ K [10]. At the Néel temperature $T_N = 38$ K, the phase transition to the antiferromagnetic state of the easy plane type occurs. As temperature decreases, the crystal spontaneously transforms from the easy-plane state into the easy-axis state at $T = 9$ K. The magnetic structure is represented by the planes alternating along axis c, perpendicular to the axis, and containing ferromagnetically ordered iron and gadolinium ions. The neighboring planes are ordered antiferromagnetically [11]. In the $NdFe_3(BO_3)_4$ crystal, the antiferromagnetic phase transition proceeds at $T_N = 30$ K [13, 14]. In addition, an anomaly was revealed, at $T = 6$ K, in the temperature dependence of the magnetic susceptibility in the ab plane perpendicular to trigonal axis c [14, 15]. In [14, 16], this anomaly is explained by a change in the level population of the ground Kramers doublet of the Nd^{3+} ions split by the magnetic field induced by the ordered subsystem of the Fe^{3+} ions. The same explanation is also given to the Schottky anomaly at $T \approx 4$ K in the temperature dependence of the heat capacity [14]. The theoretical analysis of the magnetic properties of $NdFe_3(BO_3)_4$ was performed in [17]. The neutron diffraction experiments show that the magnetic moments of the Fe^{3+} and Nd^{3+} sublattices are ordered antiferromagnetically, and they lie in the plane perpendicular to axis c [7]. In the paramagnetic region, the temperature dependences of the magnetic susceptibility along the trigonal axis and in the basal plane are identical, and they give the Weiss constant $\Theta = -110$ K [14].

In this work, the magnetic properties of the $Nd_{0.5}Gd_{0.5}Fe_3(BO_3)_4$ single crystal are studied and compared with the magnetic properties of the related $GdFe_3(BO_3)_4$ and $NdFe_3(BO_3)_4$ crystals.

2. RESULTS AND DISCUSSION

The $Nd_{0.5}Gd_{0.5}Fe_3(BO_3)_4$ single crystal was grown from a $K_2Mo_3O_{10}$-based solution–melt as described in

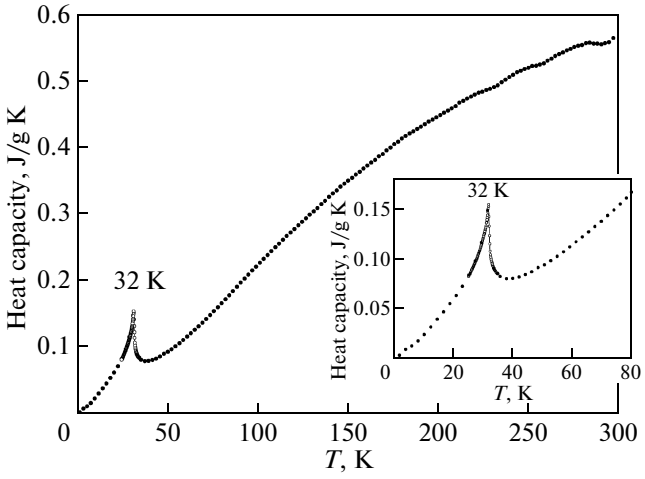

Fig. 1. Temperature dependences of the heat capacity of the $Nd_{0.5}Gd_{0.5}Fe_3(BO_3)_4$ crystal.

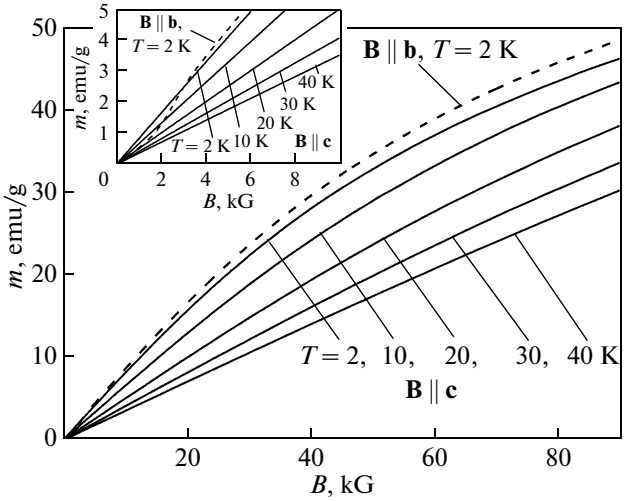

Fig. 2. Field dependences of the magnetization of the $Nd_{0.5}Gd_{0.5}Fe_3(BO_3)_4$ crystal at various temperatures.

[10]. The neodymium and gadolinium concentrations are indicated according to the proportions of corresponding oxides in the solution–melt. The structure of the crystal grown was determined using a SMART APEX-II X-ray diffractometer with a CCD detector. It was established that the structure at room temperature is identical to that of $GdFe_3(BO_3)_4$ and $NdFe_3(BO_3)_4$ crystals, i.e., it belongs to space group $R32$ and has the lattice parameters $a = 9.557(7)$ Å and $c = 7.62(1)$ Å. For comparison, at room temperature, the lattice parameters of $GdFe_3(BO_3)_4$ are $a = 9.5203(1)$ Å and $c = 7.5439(5)$ Å [9], and those of $NdFe_3(BO_3)_4$ are $a = 9.5878(3)$ Å and $c = 7.6103(3)$ Å [7]. The heat capacity and the magnetization in fields to 90 kG were measured on a Quantum Design Physical Properties Measurement System (PPMS). A part of the magnetic measurements was carried out on a Quantum Design SQUID MPMS-XL magnetometer. The temperature dependence of the heat capacity (Fig. 1) has a singularity at a temperature of 32 K corresponding to a magnetic ordering. Peculiarities corresponding to structural transitions and the Schottky anomaly were not detected.

Figure 2 shows the magnetization curves measured in a field **B** || **c** (along the trigonal axis of the crystal) at various temperatures and in a field **B** || **b** at $T = 2$ K (the *b* direction is not an axis of symmetry in the crystal; it is perpendicular to axes *c* and *a*). The magnetization curves measured in directions *a* and *b* coincide within the experimental error. According to [2], the magnetization of $NdFe_3(BO_3)_4$ in the field parallel to axis *c* is independent of temperature. It is associated in [2] with the absence of a contribution of the rare-earth subsystem; it is quite strange, since, according to [16], *g* factor of the lower doublet along axis *c* is nonzero ($g_c = 1.376$). In addition, the magnetization of $NdFe_3(BO_3)_4$ in the field **B** || **c**, at a temperature of 4.5 K, is linear in field up to 200 kG [2]. Nothing of the kind has been observed in the $Nd_{0.5}Gd_{0.5}Fe_3(BO_3)_4$ crystal (Fig. 2). This difference may be assigned to the influence of the gadolinium subsystem; however, we have no data on the behavior of the $GdFe_3(BO_3)_4$crystal in the easy-plane state in high fields.

The temperature dependence of the susceptibility in the field **B** || **c** is shown in Fig. 3. The anomaly in the region of magnetic ordering is noticeable only in the derivative of the susceptibility with respect to temperature (Fig. 3). The temperature dependences of the susceptibility measured in a field of 1 kG parallel to directions *a* and *b* clearly demonstrate features at temperatures of 11 and 33 K (Figs. 4 and 5). Similar fea-

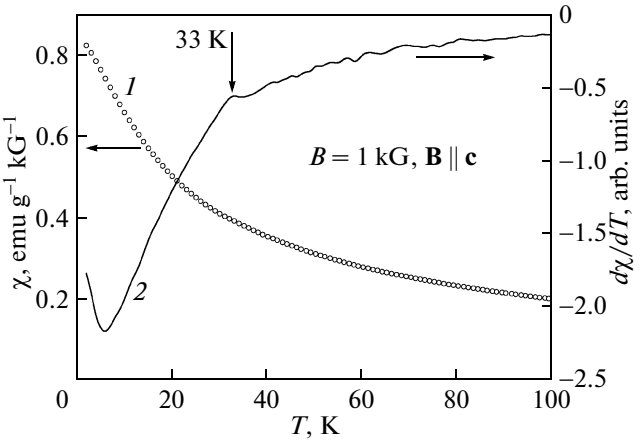

Fig. 3. Temperature dependences of (*1*) the magnetic susceptibility of the $Nd_{0.5}Gd_{0.5}Fe_3(BO_3)_4$ crystal in the magnetic field 1 kG parallel to the trigonal axis and (*2*) the derivative of the susceptibility with respect to temperature.

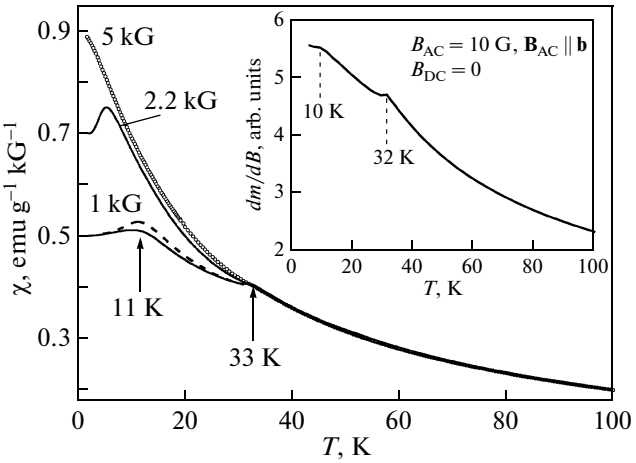

Fig. 4. Temperature dependences of the magnetic susceptibility of the $Nd_{0.5}Gd_{0.5}Fe_3(BO_3)_4$ crystal in directions *a* and *b* (dashed line) measured in various magnetic fields. The inset shows the temperature dependence of the differential susceptibility in the ac field.

tures there are at 10 and 32 K in the temperature dependence of the differential susceptibility in a weak ac field in the *ab* plane (Fig. 4, inset). (Insignificant difference in the feature positions is likely due to the influence of magnetic field.) In the field 2.2 kG, the first feature shifts to a temperature of 5.8 K, and the features in directions *a* and *b* are almost indiscernible (Fig. 4). In the field 5 kG parallel to directions *a* and *b*, the feature at 33 K is observed only in the derivative of the susceptibility with respect to temperature; the first feature disappear completely (Figs. 4 and 5), and the difference between directions *a* and *b* is lost.

The temperature behavior of the susceptibility in fields **B** ∥ **b** and **B** ∥ **c** is shown in Fig. 6. The dependences in fields **B** ∥ **a** and **B** ∥ **b** are almost identical.

The dependences obtained are deviated from the Curie–Weiss law well before the temperature of magnetic ordering. The extrapolation of the linear segments to a zero gives the Weiss parameters for two directions of the field $\Theta_c = -45$ K and $\Theta_{a,b} = -70$ K. Thus, the ordering has antiferromagnetic character, and, along with the crystallographic magnetic anisotropy, there is the anisotropy of exchange interaction (the exchange interaction is stronger in the *ab* plane). In [10, 14], for $GdFe_3(BO_3)_4$ and $NdFe_3(BO_3)_4$, only one Weiss parameter is given for all the field directions, namely, $\Theta = -115$ and -110 K, respectively. In $Nd_{0.5}Gd_{0.5}Fe_3(BO_3)_4$, the spin flop transition is not observed in a field parallel to trigonal axis *c* in the temperature range under study (Fig. 2). It means that in the free state, the magnetic moments lie in the *ab* plane, and, unlike $GdFe_3(BO_3)_4$, no spontaneous spin-reorientational transition occurs.

The magnetic susceptibility, at fairly high temperature in the paramagnetic region, is described by the relationship

$$\chi = \frac{nm_{\text{eff}}^2}{3k(T-\Theta)}. \quad (1)$$

Here, m_{eff} is the effective moment of the $Nd_{0.5}Gd_{0.5}Fe_3(BO_3)_4$ molecules, and *n* is the number of the molecules in 1 g of the crystal: $n = N/M$, where *N* is the Avogadro number, and *M* is the molecular weight. Theoretically, the total effective moment is determined as the sum of the contributions of all magnetic ions

$$m_{\text{eff}}^2 = 0.5m_{\text{eff}}^2(Nd^{3+}) + 0.5m_{\text{eff}}^2(Gd^{3+}) + 3m_{\text{eff}}^2(Fe^{3+}), \quad (2)$$

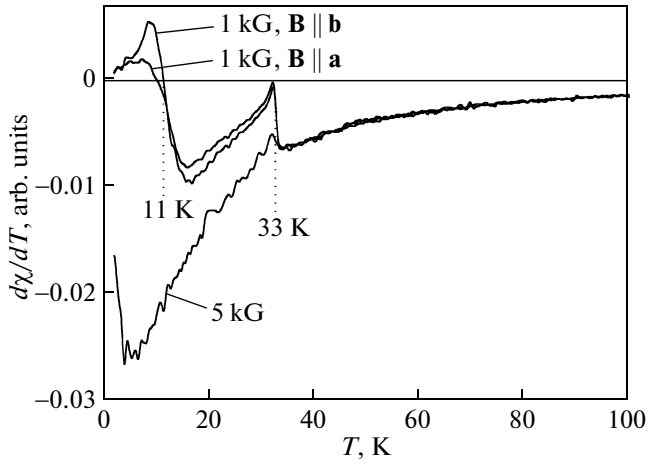

Fig. 5. Temperature dependences of the derivatives of the magnetic susceptibility of the $Nd_{0.5}Gd_{0.5}Fe_3(BO_3)_4$ crystal with respect to temperature measured in the *ab* plane.

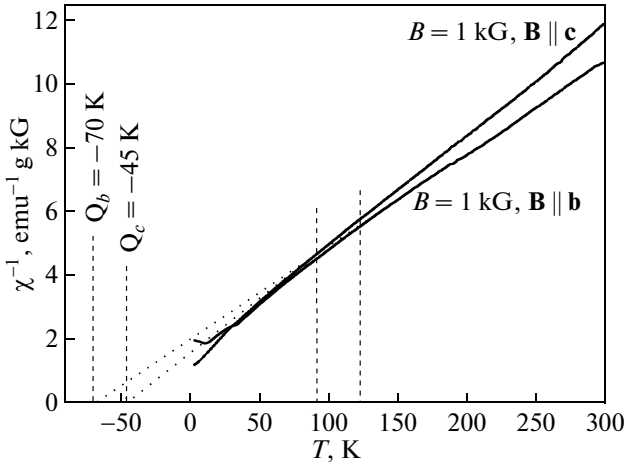

Fig. 6. Temperature dependences of the inverse magnetic susceptibilities of the $Nd_{0.5}Gd_{0.5}Fe_3(BO_3)_4$ crystal measured in the *b* and *c* directions.

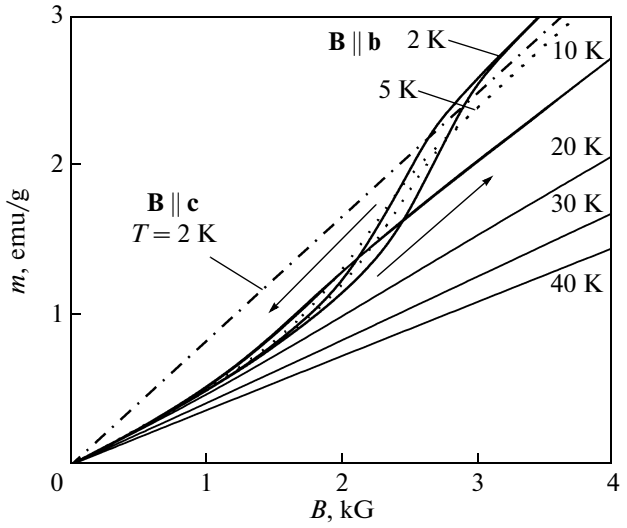

Fig. 7. Field dependences of the magnetization of the $Nd_{0.5}Gd_{0.5}Fe_3(BO_3)_4$ crystal measured in the *b* and *c* directions at various temperatures.

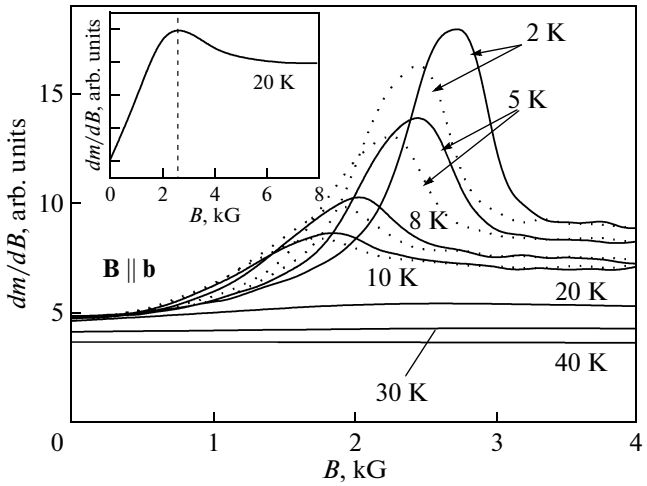

Fig. 8. Field dependences of the differential susceptibility of the $Nd_{0.5}Gd_{0.5}Fe_3(BO_3)_4$ crystal measured in the *b* direction at various temperatures. The solid lines correspond to an increase in the field, and the dotted lines, to a decrease in the field.

where $m_{\text{eff}}^2 = g^2J(J+1)$ in the Bohr magnetons. As a result, we find that $m_{\text{eff}} = 11.97$. The experimental value of m_{eff} can be found by relationship (1) using any point in the curves shown in Fig. 6 from the linearity segment and the Weiss parameters found. For two the directions of the field, we obtain $m_{\text{eff}}(c) = 11.29$ and $m_{\text{eff}}(ab) = 12.33$, and the average value is $m_{\text{eff}} = 11.81$.

In weak field (0–3.5 kG), in the *ab* plane, at $T < T_N$, the magnetization *m* is a nonlinear function of field. At a temperature $T < 11$ K, the function has hysteresis (Fig. 7). At 2 K, the hysteresis loop width is ≈0.25 kG. At the same time, in low fields in regions $B < 1$ kG and $B > 3.5$ kG, $m(B)$ are approximately linear functions; i.e., the differential susceptibility dm/dB is a constant that is nevertheless different in the noted regions (Fig. 8). In addition, the functions $m(B)$ in the regions $B < 1$ kG and $B > 3.5$ kG are the same during the direct and inverse variation of the field. It implies that, in these regions, the crystal is in different but reversible magnetic states. Figure 8 clearly demonstrates the transformation of the hysteresis loops with temperature. The temperature of appearance of the hysteresis coincides with the position of the feature in the temperature dependence of the susceptibility (Fig. 4) measured in the field $B = 1$ kG (the reversible part of the hysteresis loop) and in the temperature dependence of the differential susceptibility in the ac field 10 G, 100 Hz (Fig. 4, inset). Thus, the specific feature in the temperature dependence at $T = 11$ K is related to the appearance of the hysteresis. Earlier [18], the electric polarization hysteresis was observed during the magnetization reversal of $Nd_{0.5}Gd_{0.5}Fe_3(BO_3)_4$.

From the standpoint of symmetry, the domains with three equivalent directions of the magnetic moments (both iron, and rare-earth ions) must exist in the *ab* plane. It is impossible to indicate these directions based only on magnetic measurements. Actually, it was shown in [12] using the Mössbauer effect measurements that, in the easy-axis state of $GdFe_3(BO_3)_4$, the moments are deviated from the trigonal axis of the crystal, and, in the easy-plane state, they are deviated from the basal plane. The experiments on the neutron scattering show that the magnetic moments of the iron and neodymium sublattces in $NdFe_3(BO_3)_4$ are noncollinear, and the angle between them varies with temperature [7]. Three directions of the magnetic moments are energetically equivalent, but there is a potential barrier between corresponding domains whose value is characterized by the temperature $T = 11$ K at which the hysteresis loops appear (Figs. 4, 7, and 8). (It is likely more properly to take the temperature 10 K from the dependence of the differential susceptibility in a weak ac field.) At $B > 1$ kG, the domain walls begin to move. At the same time, as the field against decreases to $B < 1$ kG, the magnetic anisotropy energy is sufficient to return the crystal to the initial state of the equally probable distribution of the domains with three directions of the moments. In the opposite case, the initial segment of the magnetization curve would not be reproduced during reverse run of the field. At $B < 1$ kG, the domain walls are not moved, and the magnetic moments in different domains are rotated variously because of the various mutual orientation of the magnetic moments and magnetic field, and this mutual orientation is also dependent on the field directions **B** || **a** and **B** || **b**. At the same time, within the limits of measurement error, the hysteresis loops are independent of the field direction along axes

a or *b*; and the $\chi(T)$ curves also are slightly dependent on the directions of the field along axes *a* and *b* (Figs. 4 and 5). Thus, the magnetic anisotropy in the basal plane is small. In the region of the fields $1 < B < 3.5$ kG, three processes occur as follows.

(1) The domain walls move, until one energetically preferable domain forms.

(2) The vector of antiferromagnetism is rotated perpendicularly to the magnetic field (spin flop transition); in this case, this process occurs in all the domains (and domain walls), and not only in the cases as the directions of the field and vector of antiferromagnetism coincide, but at different rates. It is likely, because of this, the spin flop transition is smeared.

(3) The magnetic moments of the sublattices are rotated in the field direction.

The spin flop transition fields at various temperatures can be estimated from Fig. 8 as the average from the positions of the differential susceptibility maxima during the direct and inverse runs of the field; in particular, at 2 K, we have the field ~2.5 kG. The field decreases monotonically with increasing temperature (Fig. 8), as is the case during the spin flop transition in the easy-axis state of $GdFe_3(BO_3)_4$ [10]. In the $TbFe_3(BO_3)_4$ crystal with a strong uniaxial anisotropy, the spin flop transition field is changed with temperature in the opposite direction [19]. In [2], the spin flop transition field in the easy plane of the $NdFe_3(BO_3)_4$ crystal was estimated to be 10 kG, and, in [14], ~8 kG. At $T > 11$ K, the potential barrier between the domains is destructed by the thermal motion, and the monotonic motion of the differential susceptibility maxima is violated (Fig. 8 and the inset): instead of further decrease in the field of the maximum, it increases. At $B > 3.5$ kG, both the domain wall motion (single-domain state) and the spin flop transition are completed. Simultaneously, the feature in the temperature dependence of the magnetic susceptibility in the basal plane related to the formation of the domain structure disappears (Figs. 4 and 5), and the temperature dependences measured in the fields $\mathbf{B} \parallel \mathbf{a}$ and $\mathbf{B} \parallel \mathbf{b}$ become identical completely. This dependence is close to the temperature dependence of the susceptibility in the field $\mathbf{B} \parallel \mathbf{c}$ (Fig. 3). At $T > 11$ K, when the thermal energy exceeds the potential barrier between three equivalent directions of the magnetic moments, the three directions are equally probable in each point of the crystal at any instant of time, and the system tunnels over these states as is the case in the dynamic Jahn–Teller effect. However, the crystal state at $T < 11$ K differs from that at $T > 11$ K not only by formation of steady-state domains; new objects, namely, domains walls appear as well having different magnetic properties. In particular, the orientation of the magnetic moments and anisotropy in the domain walls and in the domains are certain to be different. It is likely, the domain walls determine different temperature dependence of the dynamic susceptibility in weak fields ($B < 1$ kG), when the domain walls still do not move, and at $B > 3.5$ kG, when the crystal transforms into the single-domain state: in weak fields, the dynamic susceptibility is unchanged at least to 11 K, and, at $B > 3.5$ kG, it decreases as temperature increases (Fig. 8). Two facts cause questions: (1) the possibility to observe the hysteresis despite a weak magnetic anisotropy in the plane, i.e., despite the magnetic identity of the domains; (2) the coincidence of the field region of existence of the hysteresis and the field region of the spin flop transition. These and other facts are likely related to the properties of the domain walls different from the properties of the domains. In particular, in weak fields ($B < 1$ kG) in which the domain walls are immobile, the appearance of the domain walls at $T = 11$ K coincides with the jump in the rate of varying the magnetic susceptibility with temperature (Figs. 4 and 5). The decrease in the jump temperature (Fig. 4) with increasing field can be explained by a decrease in the number of the domain walls and a decrease in their contribution to the magnetic properties of the crystal.

3. CONCLUSIONS

The heat capacity has been measured in the range 2–300 K. The magnetic properties have been studied in the principal crystallographic directions in fields to 90 kG and in the temperature range 2–300 K. At a temperature of 32 K the transition to the antiferromagnetic easy-plane state was detected; this state is retained to $T = 2$ K. From the temperature dependences of the magnetic susceptibility in the paramagnetic region, we determined various Weiss parameters $\Theta_c = -45$ and $\Theta_{ab} = -70$ in the fields parallel and perpendicular to the third-order axis of the crystal and the corresponding effective magnetic moments $m_{\text{eff}}(c) = 11.29$ and $m_{\text{eff}}(ab) = 12.33$. The hysteresis was revealed during magnetization of the crystal in the easy plane perpendicular to the third-order axis of the crystal in the field range 1–3.5 kG; and the spin flop transition was also detected occurring at a temperature of 2 K in a field of ~2.5 kG. At a temperature of 11 K, in fields $B < 1$ kG, there is a peculiarity in the temperature dependence of the susceptibility in the easy plane. At the same temperature, the hysteresis noted above appears: i.e., at higher temperature, the thermal energy is sufficient to overcome the potential barrier between the domains with three energetically equivalent directions of the magnetic moments, and the crystal tunnels between these states in each point. In fields $B > 3.5$ kG, the crystal transforms into the single-domain state, and the peculiarity in the temperature dependence of the susceptibility disappears. Thus, the peculiarity is related to the formation of the steady-state domains, and, thus, steady-state domain walls. It is precisely the existence of the steady-state domain walls that differs the crystal state at $T < 11$ K from the state at $T > 11$ K. The behavior of the susceptibility in

fields 1–3.5 kG is determined by motion of the domain walls and also by spin flop transitions and rotation of the magnetic moments in the magnetic field direction not only in the domains but also in the domain walls. The magnetic properties of the $Nd_{0.5}Gd_{0.5}Fe_3(BO_3)_4$ crystal is substantially different as compared to the magnetic properties of both $NdFe_3(BO_3)_4$ and $GdFe_3(BO_3)_4$.

ACKNOWLEDGMENTS

This study was supported by the Russian Foundation for Basic Research, project no. 09-02-00171-a.

REFERENCES

1. A. K. Zvezdin, S. S. Krotov, A. M. Kadomtseva, G. P. Vorob'ev, Yu. F. Popov, A. P. Pyatakov, L. N. Bezmaternykh, and E. A. Popova, JETP Lett. **81** (6), 272 (2005).
2. A. K. Zvezdin, G. P. Vorob'ev, A. M. Kadomtseva, Yu. F. Popov, A. P. Pyatakov, L. N. Bezmaternykh, A. V. Kuvardin, and E. A. Popova, JETP Lett. **83** (11), 509 (2006).
3. F. Yen, B. Lorenz, Y. Y. Sun, C. W. Chu, L. N. Bezmaternykh, and A. N. Vasiliev, Phys. Rev. B: Condens. Matter **73**, 054435 (2006).
4. A. M. Kadomtseva, Yu. F. Popov, G. P. Vorob'ev, A. A. Mukhin, V. Yu. Ivanov, A. M. Kuz'menko, and L. N. Bezmaternykh, JETP Lett. **87** (1), 39 (2008).
5. R. P. Chaudhury, F. Yen, B. Lorenz, Y. Y. Sun, L. N. Bezmaternykh, V. L. Temerov, and C. W. Chu, Phys. Rev. B: Condens. Matter **80**, 104424 (2009).
6. A. N. Vasiliev and E. A. Popova, Low Temp. Phys. **32** (8), 735 (2006).
7. P. Fischer, V. Pomjakushin, D. Sheptyakov, L. Keller, M. Janoschek, B. Roessli, J. Schefer, G. Petrakovskii, L. Bezmaternikh, V. Temerov, and D. Velikanov, J. Phys.: Condens. Matter **18**, 7975 (2006).
8. R. Z. Levitin, E. A. Popova, R. M. Chtshebrov, A. N. Vasiliev, M. N. Popova, E. P. Chukalina, S. A. Klimin, P. H. M. van Loosdrecht, D. Fausti, and L. N. Bezmaternykh, JETP Lett. **79** (9), 423 (2004).
9. S. A. Klimin, D. Fausti, A. Meetsma, L. N. Bezmaternykh, P. H. M. van Loosdrecht, and T. T. M. Palstra, Acta Crystallogr., Sect. B: Struct. Sci. **61**, 481 (2005).
10. A. D. Balaev, L. N. Bezmaternykh, I. A. Gudim, V. L. Temerov, S. G. Ovchinnikov, and S. A. Kharlamova, J. Magn. Magn. Mater. **258–259**, 532 (2003).
11. A. I. Pankrats, G. A. Petrakovskii, L. N. Bezmaternykh, and O. A. Bayukov, JETP **99** (4), 766 (2004).
12. S. A. Kharlamova, S. G. Ovchinnikov, A. D. Balaev, M. F. Tomas, I. S. Lyubutin, and A. G. Gavriliyuk, JETP **101** (6), 1098 (2005).
13. N. Tristan, R. Klingeler, C. Hess, B. Büchner, E. Popova, I. A. Gudim, and L. N. Bezmaternykh, J. Magn. Magn. Mater. **316**, e621 (2007).
14. E. A. Popova, N. Tristan, C. Hess, R. Klingeler, B. Büchner, L. N. Bezmaternykh, V. L. Temerov, and A. N. Vasil'ev, JETP **105** (1), 105 (2007).
15. J. A. Campá, C. Cascales, E. Gutiérrez-Puebla, M. A. Monge, I. Rasines, and C. Ruíz-Valero, Chem. Mater. **9**, 237 (1997).
16. M. N. Popova, E. P. Chukalina, T. N. Stanislavchuk, B. Z. Malkin, A. R. Zakirov, E. Antic-Fidancev, E. A. Popova, L. N. Bezmaternykh, and V. L. Temerov, Phys. Rev. B: Condens. Matter **75**, 224435 (2007).
17. D. V. Volkov, A. A. Demidov, and N. R. Kolmakova, JETP **104** (6), 897 (2007).
18. A. M. Kadomtseva, Yu. F. Popov, G. P. Vorob'ev, A. A. Mukhin, V. Yu. Ivanov, A. M. Kuz'menko, A. S. Prokhorov, L. N. Bezmaternykh, V. L. Temerov, and I. A. Gudim, in *Proceedings of the XXI International Conference "New in Magnetism and Magnetic Materials," Moscow, 2009*, p. 316.
19. C. Ritter, A. Balaev, A. Vorotynov, G. Petrakovskii, D. Velikanov, V. Temerov, and I. Gudim, J. Phys.: Condens. Matter **19**, 196227 (2007).

Translated by Yu. Ryzhkov